Connectivity-Aware Task Offloading for Remote Northern Regions: a Hybrid LEO-MEO Architecture

Mohammed Almekhlafi*, Antoine Lesage-Landry*[‡], Gunes Karabulut Kurt*

*Department of Electrical Engineering, Polytechnique Montréal & Poly-Grames Research Centre, QC, Canada

[‡]Department of Electrical Engineering, Polytechnique Montréal, Mila & GERAD, Montréal, QC, Canada

Emails: {mohammed.al-mekhlafi, antoine.lesage-landry, gunes.kurt}@polymtl.ca

Abstract-Arctic regions, such as northern Canada, face significant challenges in achieving consistent connectivity and lowlatency computing services due to the sparse coverage of Low Earth Orbit (LEO) satellites. To enhance service reliability in remote areas, this paper proposes a hybrid satellite architecture for task offloading that combines Medium Earth Orbit (MEO) and LEO satellites. We develop an optimization framework to maximize task offloading admission rate while balancing the energy consumption and delay requirements. Accounting for satellite visibility and limited computing resources, our approach integrates dynamic path selection with frequency and computational resource allocation. Because the formulated problem is NP-hard, we reformulate it into a mixed-integer convex form using disjunctive constraints and convex relaxation techniques, enabling efficient use of off-the-shelf optimization solvers. Simulation results show that, compared to a standalone LEO network. the proposed hybrid LEO-MEO architecture improves the task admission rate by 15% and reduces the average delay by 12%. These findings highlight the architecture's potential to enhance connectivity and user experience in remote Arctic areas.

Keywords—Low Earth orbit, medium Earth orbit, task offloading, non-terrestrial networks.

I. INTRODUCTION

With the growing demand for global and seamless connectivity, non-terrestrial networks (NTNs) are anticipated to play a key role in extending coverage to remote, rural, and underserved regions [1]-[4]. This is reinforced by the broad coverage provided by various satellite types within NTNs, including geostationary orbit (GEO), medium Earth orbit (MEO), and low Earth orbit (LEO) satellites [1]. The next-generation satellites, particularly those in LEOs and MEOs, offer significantly higher throughput and lower latency compared to traditional systems, thereby enabling support for a wide range of 6G applications. As a result, NTNs are becoming a crucial component in realizing the vision of future 6G networks [3]. In line with this vision, the 3rd Generation Partnership Project (3GPP) has been actively engaged in standardizing NTNs, with a focus on aspects such as the integration of onboard mobile edge computing (MEC) capabilities [4].

MEC has demonstrated its effectiveness in terrestrial communication by significantly reducing end-to-end latency by

This work was supported in part by Fonds de recherche du Québec secteur Nature et technologies (FQRNT) and the Natural Sciences and in part by Engineering Research Council (NSERC) of Canada Alliance grant ALLRP 579869-22 ("Artificial Intelligence Enabled Harmonious Wireless Coexistence for 3D Networks (3D-HARMONY)").



Fig. 1: Starlink network: Northern Canada. Adapted from [9]. allocating computational resources closer to the network edge [5], [6]. This proximity enables real-time processing for users, particularly those with limited computational capabilities, and is especially beneficial for time-sensitive or resource-intensive tasks. Building on advancements in terrestrial mobile edge computing, several studies have explored the potential of LEO satellites for edge computing. Although LEO satellites present considerable benefits for task offloading, their deployment is constrained in certain areas, such as northern Canada, where networks like Starlink are sparsely distributed and insufficient to provide comprehensive coverage, as illustrated in Fig. 1. These challenges are further intensified by cost considerations, as the low population density in these regions makes largescale deployments economically unfeasible. In such cases, limited coverage and frequent outages can undermine efforts to provide reliable communication, which has been identified as a basic human right [7]. Also, many studies have highlighted access inequality in remote areas, such as northern Canada, calling for effective solutions to address this issue [8].

Given the limitations of LEO satellites in remote Arctic areas, this work explores the relationship between connectivity and computational efficiency in hybrid LEO-MEO networks. With broader coverage and moderate latency, MEO satellites can help mitigate LEO network limitations. In other words, MEO satellites have a longer visibility period than LEO satellites, which helps maintain continuity of service despite their higher propagation delay. The primary contributions of this work are as follows

 We studied task offloading in hybrid LEO-MEO satellite networks. To achieve this, we formulate an optimization problem that maximizes the number of offloaded tasks while balancing the total delay and energy consumption, ensuring QoS requirements are met. We consider

- optimizing computational and frequency resources while incorporating a dynamic round-trip migration strategy.
- Because the problem is NP-hard, we employ disjunctive constraints and convex relaxations to transform it into a mixed-integer convex problem that can be solved using standard optimization tools.
- We demonstrate the benefits of the proposed hybrid LEO-MEO scheme through extensive numerical simulations and using a realistic Starlink network model combined with an MEO satellite orbital configuration. Our results show that the proposed hybrid LEO-MEO scheme enhances user experience by increasing the task admission rate by up to 15% and reducing the average delay by up to 12% compared to the baseline.

II. RELATED WORKS

Task offloading has been extensively studied in both terrestrial and aerial networks across various applications and scenarios [10]–[17]. The authors of [12] introduce UAVs to address the overloading issue in vehicular edge computing networks. The formulated problem aims to minimize the average task delay while being constrained by the energy consumption of unmanned aerial vehicles (UAVs). In [13], self-learning solutions are proposed to decide whether the task should be offloaded to the edge or executed by the UAVs to balance between the power consumption of the vehicles and task delays. Similar problem and distributed learning are considered in [14] for the multi-cell and multi-UAV setup.

Ren et al. [11] focuses on reducing system delay by integrating HAPS while optimizing key factors such as task offloading, service caching, and computational resource distribution. They utilize the value decomposition network (VDN) method to develop an effective decision-making process. Additionally, the authors of [10] propose two multi-connectivity offloading solutions to improve the probability of timely task completion by efficiently distributing tasks between high-altitude platform stations (HAPS) and UAVs. A task partitioning scheme is introduced in [17], where the task is divided into three portions and processed in parallel at the vehicle, roadside units, and a HAPS. Because the problem is not convex, a variable replacement and the successive convex approximation method are used to solve the problem.

Task offloading optimization for NTNs is studied in [18]–[23]. The authors of [18] introduce a general framework for LEO satellite-assisted task offloading, targeting real-time, high-resolution Earth observations. They suggest an iterative optimization approach, focusing on the optimal selection of data allocation, compression ratio, and processing frequency. The work in [20] explores distributed task offloading optimization within multi-agent networks, aiming to maximize the successful offloading rate of agents. The problem is reformulated into an unconstrained optimization problem, and game theory is applied to solve it. In [21], the aggregation latency in a multi-hop scheme is studied where the tasks can be performed at the cloud or the LEO network. A multi-layered LEO constellation combined with terrestrial components is considered

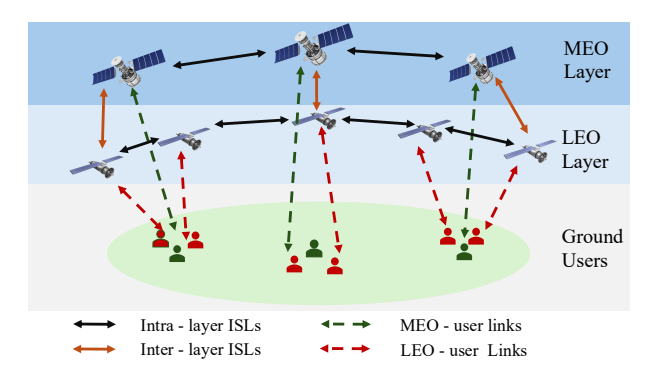


Fig. 2: Multi-layer task offloading system model.

in [22], where the authors formulate a network selection problem to minimize latency costs. In [23], duelling double deep-Q-learning (D3QN) algorithm is proposed to reduce service delay for task migration in LEO networks. In [19], a multi-agent reinforcement learning scheme is proposed for task offloading in the Internet of Remote Things by integrating double deep Q-network (DDQN) and deep deterministic policy gradient (DDPG) to enhance decision-making efficiency and offloading performance. The connectivity challenges in Arctic regions, particularly through the use of MEO satellites, remain unaddressed. Hence, there is a clear gap in studying the benefits of integrating MEO satellites with existing LEO networks for task offloading, which is the focus of this paper.

III. SYSTEM MODEL

We consider sets of LEO and MEO satellites, denoted by $\mathcal{L} = \{1, 2, \dots, L\}$ and $\mathcal{N} = \{1, 2, \dots, N\}$, respectively, where $L \in \mathbb{N}$ and $N \in \mathbb{N}$ is the total number of LEO and MEO satellites, respectively. We assume that these satellites are moving within fixed orbits. The satellites provide communication services to a set of users, denoted by $\mathcal{U} = \{1, 2, \dots, U\},\$ where $U \in \mathbb{N}$ is the number of users located in an isolated region without access to terrestrial networks, such as Northern Canada which we consider in this work. We assume that these satellites are equipped with MEC servers, making them capable of handling computational tasks generated by ground users. Moreover, the satellites can communicate through intersatellite links (ISL), and offloaded tasks can be relayed to their neighbouring LEO or MEO counterparts. In this context, we model the satellite network as the graph $\mathcal{G}(\mathcal{S}, \mathcal{E})$, where $\mathcal{S} \triangleq \mathcal{N} \cup \mathcal{L} = \{1, 2, \dots, L+N\}$ is the set of nodes representing the satellites and \mathcal{E} is the set of edges representing the ISL links between satellites. Then, if the computation resources of a satellite are insufficient to process a task, it can be forwarded to a neighbouring LEO or MEO satellite. Likewise, if a user moves out of the assigned satellite's coverage, the computation results are sent to a nearby LEO or MEO satellite for continued coverage.

For mathematical convenience, let $\mathcal{K} = \{1, 2, \dots, K\}$ be the set of shortest paths, i.e., multi-hop routing, between all network node pairs. Each path is modelled as a tuple $\{d_k, s_k, \hat{s}_k\}$, where d_k is the path distance in meters, $s_k \in \mathcal{N}$ is the source satellite, and $\hat{s}_k \in \mathcal{N}$ is the destination satellite.

Without loss of generality, the frequency domain is divided into resource blocks each of bandwidth W. Let B_s denote the number of frequency resources of satellite $s \in \mathcal{S}$. For user $u \in \mathcal{U}$, the task is modelled as a tuple $\Omega_u = \{\zeta_u, X_u, \tau_u^{\max}\}\$, where ζ_u , X_u , and τ_u^{max} represent the packet size in bits, the required computation resources to complete the task in cycles/second, and the time needed to complete the task, respectively. Because satellites are moving at high speeds, each satellite is visible for a short period based on its speed and elevation angle. To account for orbital dynamics, we define the visibility duration of satellite s for user u as a tuple $v_{u,s} = \{v_{u,s}^{\text{start}}, v_{u,s}^{\text{end}}\}$, where $v_{u,s}^{\text{start}}$ and $v_{u,s}^{\text{end}}$ are the start and end times of the visibility period.

A. Routing Model

Due to satellites' mobility, users may occasionally move out of the visibility range of the satellite they are initially associated with. Consequently, both the task itself and its corresponding computation results may need to be routed through alternative paths to ensure continuity of service. This dynamic network topology results in satellites changing positions and visibility and necessitates a flexible routing mechanism. To address this, we introduce two optimization variables that enable effective routing management for task offloading and the subsequent delivery of computation results. The first variable controls the task offloading path (OP), ensuring that tasks are directed to a satellite capable of handling the computational load. The second variable is dedicated to computation results forwarding path (FP), ensuring the results reach the user even if the initial satellite association is no longer visible.

Let $i_{u,k}$ represent the offloading decision for each user ualong a specific path k. Specifically, $i_{u,k} = 1$ if the task generated by user u is offloaded through path k; otherwise, $i_{u,k} = 0$. When $i_{u,k} = 1$, user u is thereby associated with satellite s_k as the communication node, while the computational processing of the task is conducted at the destination satellite \hat{s}_k . Similarly, we introduce the binary variable $y_{u,k}$ to control the routing of the computation results. Here, $y_{u,k} = 1$ indicates that the results for user u are forwarded along path k, while $y_{u,k} = 0$ implies that path k is not used for result forwarding. Because each ground user uses only a single OP and a single FP, the following constraints must be satisfied:

$$\sum_{k \in \mathcal{K}} i_{u,k} \le 1, \forall u \in \mathcal{U}, \tag{1}$$

$$\sum_{k \in \mathcal{K}} i_{u,k} \le 1, \forall u \in \mathcal{U},$$

$$\sum_{k \in \mathcal{K}} y_{u,k} \le 1, \forall u \in \mathcal{U}.$$
(1)

To ensure a closed-loop path, whereby the task is forwarded from the destination satellite of the OP to the user through FP, the following constraint must hold:

$$\sum_{\hat{k} \in \mathcal{K}} \mathbb{I}_{s_{\hat{k}} = \hat{s}_k} \ y_{u,k} \geq i_{u,k} \ , \forall u \in \mathcal{U}, \forall k \in \mathcal{K}, \qquad (3)$$
 where $\mathbb{I}_{x_1 = x_2}$ is the indicator function, such that $\mathbb{I}_{x_1 = x_2} = 1$ if the subscript statement holds true, and 0 otherwise.

B. Communication Model

We consider that the satellites and the users are equipped with a single antenna, and the communication links between users and satellites are orthogonal. As a result, frequency resources are split orthogonally and allocated to each user. Accordingly, let b_{u,k,s_k} represent the fraction of frequency resources allocated to the u-th user by satellite s_k , where $0 \leq b_{u,k,s_k} \leq 1$. To ensure the allocated frequency resources do not exceed the capacity of each satellite, the following constraint must hold:

$$\sum_{u \in \mathcal{U}} \sum_{k \in \mathcal{K}} b_{u,k,s_k} \le 1, \, \forall s_k \in \mathcal{S}. \tag{4}$$

 $\sum\nolimits_{u\in\mathcal{U}}\sum\nolimits_{k\in\mathcal{K}}b_{u,k,s_k}\leq 1,\,\forall s_k\in\mathcal{S}. \tag{4}$ Because the frequency allocation variable is linked with the OP selection variable, the following constraint must be satisfied:

$$i_{u,k} \ge b_{u,k,s_k}, \forall u \in \mathcal{U}, \forall k \in \mathcal{K}, \forall s_k \in \mathcal{S}.$$
 (5)

The transmission rate of the u-th user through path $k \in \mathcal{K}$ is expressed as [24]:

$$R_{u,k} = b_{u,k,s_k} B_{s_k} r_{u,s_k}, \forall u \in \mathcal{U},$$
 (6)

where $\mathbf{r}_{u,s_k} = W \log_2\left(1 + \frac{p_u \, h_{u,s_k}}{\sigma_0^2}\right)$. Here, h_{u,s_k} denotes the channel gain between the u-th user and satellite s_k , p_u denotes the transmit power of the user, and σ_0^2 represents the Gaussian noise power [25].

C. Computational Model

The task is computed at the destination satellite of the forward path. Then, let f_{u,k,\hat{s}_k} be the portion of computing resources of satellite \hat{s}_k allocated to task Ω_u . It should satisfy

$$\bar{\mathbf{F}}_s + \sum_{u \in \mathcal{U}} \sum_{k \in \mathcal{U}} f_{u,k,\hat{s}_k} \, \mathbb{I}_{s_{\hat{k}} = s} \le 1, \, \forall s \in \mathcal{S}, \quad (7)$$

$$I_{u,k} \ge f_{u,k,\hat{s}_k}, \, \forall u \in \mathcal{U}, \forall k \in \mathcal{K},$$
 (8)

where $\bar{\mathbf{F}}_s$ is the portion of occupied resources. Constraint (8) guarantees that no computing resources are allocated if the OP k is not used to forward the computing task.

D. Delay and Energy Model

We now delve into the various sources of delay encountered in the proposed computing and communication models, which are summarized as follows:

a) Transmission delay: ISLs provide high transmission rates. The resulting ISL transmission delays are negligible compared to other delay components; hence, it can be ignored in the analysis [19], [26]. Furthermore, the size of the computation results of the tasks is assumed to be small, allowing us to neglect their transmission delays as well. Therefore, we focus exclusively on the time required to transmit the task from the ground user to the satellite. For path k, the transmission time $\tau_{u,k}^{\rm tr}$ and the transmit energy consumption $\rho_{u,k}^{\rm tr}$ of user u are:

$$\tau_{u,k}^{\text{tr}} = \frac{\zeta_u}{R_{u,k}}, \forall u \in \mathcal{U}, \forall k \in \mathcal{K},$$
(9)

$$\rho_{u,k}^{\mathrm{tr}} = \frac{p_u \, \zeta_u \, i_{u,k}}{\mathrm{r}_{u,s_k}}, \forall u \in \mathcal{U}, \forall k \in \mathcal{K}. \tag{10}$$
 b) Task computation delay: Offloaded tasks can be

processed at the OP destination satellite. For the task Ω_u of user $u \in \mathcal{U}$, the computational time, $au_{u,k}^{\mathrm{comp}}$, and energy consumption, $\rho_{u,k}^{\text{comp}}$, can be expressed as:

$$\tau_{u,k}^{\text{comp}} = \frac{X_u}{f_{u,k,\hat{s}_k} F_s}, \forall u \in \mathcal{U}, \forall k \in \mathcal{K},$$
(11)

$$\rho_{u,k}^{\text{comp}} = \kappa X_u f_{u,k,\hat{s}_k}^2 F_{s_k}^2, \forall u \in \mathcal{U}, \forall k \in \mathcal{K},$$
 (12)

where κ is the effective switch capacitance that depends on the chip architecture [18].

c) Propagation delay: Such delay occurs when a task or its results need to be forwarded to a neighbouring satellite due to one of the following reasons: (1) insufficient computing resources on the associated satellite and/or (2) user moving out of the coverage area because of the mobility of LEO or MEO satellites. Thus, the propagation delay is composed of the task propagation delay from the user to the associated satellite plus OP delay, $\tau_{u,k}^{\text{prop},\text{OP}}$, the delay of forwarding the task computational results to the end-user, $\tau_{u,k}^{\text{prop},\text{FP}}$, defined as:

$$\tau_{u,k}^{\text{prop,OP}} = i_{u,k} \frac{d_{u,s_k} + d_k}{c}, \forall u \in \mathcal{U}, \forall k \in \mathcal{K},$$
(13)

$$\tau_{u,k}^{\text{prop,FP}} = y_{u,k} \frac{d_{\hat{s}_k,u} + d_k}{c}, \forall u \in \mathcal{U}, \forall k \in \mathcal{K},$$
(14)

where c is the speed of light.

Taking into account all delay components, the total delay of a task Ω_u should satisfy the delay constraint as follows

$$\sum_{k \in \mathcal{K}} \tau_{u,k}^{\text{tr}} + \tau_{u,k}^{\text{prop,OP}} + \tau_{u,k}^{\text{prop,FP}} + \tau_{u,k}^{\text{comp}} \le \tau_u^{\text{max}}, \, \forall u \in \mathcal{U}. \quad (15)$$

Then, to guarantee task completion, the users should be visible to satellites during uplink and downlink transmissions. This is ensured through:

$$v_{u,s_k}^{\text{end}} i_{u,k} \mathbb{I}_{v_{u,s_k}^{\text{end}} \le 0} \ge \tau_{u,k}^{\text{tr}} + i_{u,k} \frac{d_{u,s_k}}{c}, \forall u \in \mathcal{U}, \forall k \in \mathcal{K}, \quad (16)$$

$$v_{u,\hat{s}_k}^{\text{end}} y_{u,k} \ge \sum_{\hat{k} \in \mathcal{K}} \left(\tau_{u,\hat{k}}^{\text{tr}} + \tau_{u,\hat{k}}^{\text{prop,OP}} + \tau_{u,\hat{k}}^{\text{comp}} \right) + \tau_{u,k}^{\text{prop,FP}}, \forall u \in \mathcal{U}, \forall k \in \mathcal{K},$$
 (17)

$$v_{u,\hat{s}_k}^{\text{start}} y_{u,k} \le \sum_{\hat{k} \in \mathcal{K}} \left(\tau_{u,\hat{k}}^{\text{tr}} + \tau_{u,\hat{k}}^{\text{prop,OP}} + \tau_{u,\hat{k}}^{\text{comp}} \right), \forall u \in \mathcal{U}, \forall k \in \mathcal{K}, \quad (18)$$

where $\mathbb{I}_{v_{u,s_k}^{\mathrm{end}} \leq 0} = 1$ if user u is visible to satellite s_k at transmission time and 0 otherwise.

IV. PROBLEM FORMULATION

In this paper, our objective is to maximize the admitted tasks while promoting the effective use of computation and frequency resources. To achieve this, we consider the following objective function

$$\eta(\mathbf{I}, \mathbf{Y}, \mathbf{F}, \mathbf{B}) = \sum_{u \in \mathcal{U}} \sum_{k \in \mathcal{K}} i_{u,k} - \alpha_1 \sum_{u \in \mathcal{U}} \frac{\sum_{k \in \mathcal{K}} (\rho_{u,k}^{tr} + \rho_{u,k}^{\text{comp}})}{\rho_{u}^{\text{max}}} \\
-\alpha_2 \sum_{u \in \mathcal{U}} \frac{\sum_{k \in \mathcal{K}} (\tau_{u,k}^{\text{tr}} + \tau_{u,k}^{\text{prop,OP}} + \tau_{u,k}^{\text{prop,FP}} + \tau_{u,k}^{\text{comp}})}{\tau_{u}^{\text{max}}},$$
(19)

where the normalization factor $\rho_u^{\rm max}$ is the maximum power consumption for offloading task of user u. This function accounts for the number of admitted tasks while balancing between energy consumption and transmission delay by incorporating the weighting parameters $\alpha_1,\alpha_2\in[0,1]$. These parameters allow for adjustable emphasis on energy efficiency versus delay minimization, depending on system requirements. The final problem is formulated as follows:

$$\mathcal{P}_1: \quad \max_{\mathbf{I}, \mathbf{Y}, \mathbf{F}, \mathbf{B}} \eta(\mathbf{I}, \mathbf{Y}, \mathbf{F}, \mathbf{B}) \tag{20a}$$

s.t.
$$(1) - (3), (4), (5), (7), (8), (15) - (18),$$
 (20b)

$$0 \le b_{u,k,s_k} \le 1, \forall u \in \mathcal{U}, \forall k \in \mathcal{K}, \forall s_k \in \mathcal{S}, \quad (20c)$$

$$0 \le f_{u,k,\hat{s}_k} \le 1, \forall u \in \mathcal{U}, \forall k \in \mathcal{K}, \forall s_k \in \mathcal{S}, \quad (20d)$$

$$i_{u,k}, y_{u,k} \in \{0,1\}, \forall u \in \mathcal{U} \,\forall k \in \mathcal{K}.$$
 (20e)

Problem \mathcal{P}_1 is a non-convex mixed-integer non-linear programming (MINLP) problem, making it challenging to solve directly. Particularly, objective (20a) and constraints (15)–(18) are not convex due to the term $\frac{1}{x}$ which is not convex for $x \geq 0$, where x represents b_{i,k,s_k} and f_{i,k,\hat{s}_k} .

V. SOLUTION APPROACH

In this section, we present our methodology for (mixed-integer) convexifying the non-convex objective and constraints of \mathcal{P}_1 . We refer to a problem as mixed-integer convex when relaxing its integer variables to continuous ones yields a convex optimization problem. We begin by introducing auxiliary variables ϑ_{u,k,s_k} and φ_{u,k,\hat{s}_k} representing the fraction of bandwidth and frequency resources allocated to the u-th user in the k-th path at both access and destination nodes respectively, which can be written as:

$$\vartheta_{u,k,s_k} \ge \frac{1}{b_{u,k,s_k}}, \forall u \in \mathcal{U}, \forall k \in \mathcal{K}, \forall s_k \in \mathcal{S},$$
(21)

$$\varphi_{u,k,\hat{s}_k} \ge \frac{1}{f_{u,k,\hat{s}_k}}, \forall u \in \mathcal{U}, \forall k \in \mathcal{K}, \forall \hat{s}_k \in \mathcal{S}.$$
 (22)

$$\varphi_{u,k,\hat{s}_k}, \vartheta_{u,k,s_k} \geq 0, \forall u \in \mathcal{U}, \forall k \in \mathcal{K}, \forall \hat{s}_k \in \mathcal{S}.$$
 (23)

Then, transmission and computing delays are expressed as

$$\tau_{u,k}^{\text{tr}} = \frac{\zeta_u \,\vartheta_{u,k,s_k}}{B_{s_k} \, r_{u,s_k}}, \forall u \in \mathcal{U}, \forall k \in \mathcal{K}, \tag{24}$$

$$\tau_{u,k}^{\text{comp}} = \frac{X_u \, \varphi_{u,k,\hat{s}_k}}{F_s}, \forall u \in \mathcal{U}, \forall k \in \mathcal{K}.$$
 (25)

By introducing these auxiliary variables, we reformulate the original non-convex constraints, namely constraints (15)-(18), into upper bound convex (affine) forms. Consequently, the objective function becomes concave, as confirmed by the Hessian matrix, which is negative semidefinite. Specifically, the second derivative is $-2\kappa X_u F_x^2$ with respect to \mathbf{F} and zero otherwise. The definiteness of the Hessian matrix ensures that the reformulated problem has a concave objective function, making its maximization tractable. However, constraints (21) and (22) remain non-convex due to the potential division by zero for frequency and computing resources allocation, which occurs if a task is not offloaded. To address this issue, we adopt disjunctive (Big-M) constraints as follows

$$\vartheta_{u,k,s_k} \le M_1 i_{u,s}, \forall u \in \mathcal{U}, \forall k \in \mathcal{K}, \forall s_k \in \mathcal{S},$$
 (26)

$$\vartheta_{u,k,s_k} \ge \frac{1}{b_{u,k,s_1} + \epsilon_1} - (1 - i_{u,k}) \mathcal{M}_1, \forall u \in \mathcal{U}, \forall k \in \mathcal{K}, \forall s_k \in \mathcal{S},$$
 (27)

$$\varphi_{u,k,\hat{s}_k} \le M_2 i_{u,k}, \forall u \in \mathcal{U}, \forall k \in \mathcal{K}, \forall \hat{s}_k \in \mathcal{S},$$
 (28)

$$\varphi_{u,k,\hat{s}_k} \ge \frac{1}{f_{u,k,\hat{s}_k} + \epsilon_2} - (1 - i_{u,k}) \mathcal{M}_2, \forall u \in \mathcal{U}, \forall k \in \mathcal{K}, \forall \hat{s}_k \in \mathcal{S}.$$
 (29)

Here, M_1 and M_2 denote a sufficiently large constants, while ϵ_1 and ϵ_2 are a very small positive number. These parameters are chosen to ensure that $\vartheta_{u,k,s_k}=0$ and $\varphi_{u,k,\hat{s}_k}=0$ when the task is not offloaded and greater than zero if the task is offloaded. Finally, problem \mathcal{P}_1 can be written as,

$$\mathcal{P}_2: \max_{\mathbf{I}, \mathbf{Y}, \mathbf{F}, \mathbf{B}, \boldsymbol{\vartheta}, \boldsymbol{\varphi}} \eta(\mathbf{I}, \mathbf{Y}, \mathbf{F}, \mathbf{B}, \boldsymbol{\vartheta}, \boldsymbol{\varphi})$$
 (30a)

s.t.
$$(20b) - (20e), (23), (26) - (29).$$
 (30b)

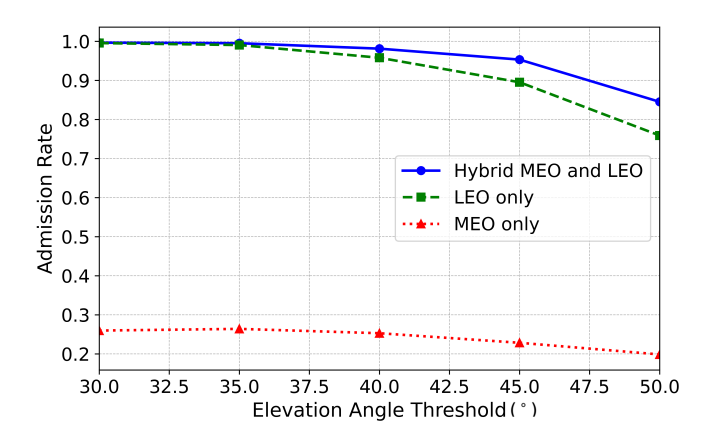
Problem \mathcal{P}_2 is convex mixed-integer non-linear program (MINLP), allowing us to use various off-the-shelf tools, such as cvxpy [27] and Gurobi [28]. The overall complexity depends on the chosen solver and algorithm [29].

VI. EVALUATION OF THE PROPOSED ARCHITECTURE

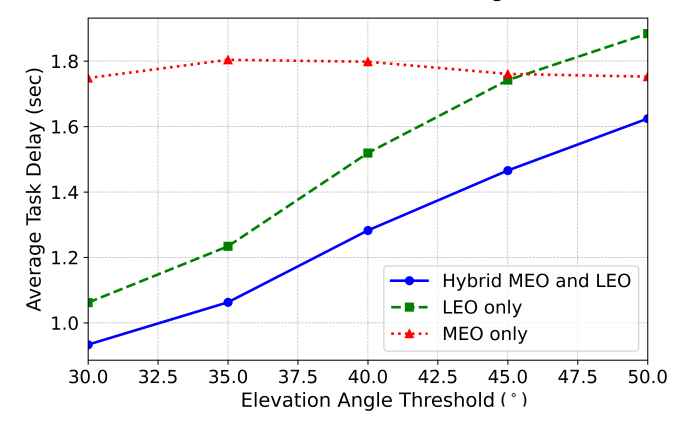
In this section, we present comprehensive numerical results to assess the performance of the proposed offloading scheme using a Python-based simulator. Specifically, the Skyfield package [30] is employed to model the deployment of LEO satellites, simulating the Starlink constellation through the adoption of the latest two-line element (TLE) set [31]. This data enables accurate estimation of the position and velocity of Starlink satellites. Additionally, the simulation includes 30 MEO satellites positioned at an altitude of 2100 km, distributed across three orbital planes with inclination angles of 86°, 88°, and 90°, forming near-polar orbits. The MEO satellites are deployed to enhance coverage in the northern region of Québec, Canada, particularly around Ivujivik (latitude 62°, longitude -77.5°). The LEO and MEO satellites are also assumed to have 25 and 50 frequency resources, respectively, with each resource block of 180 kHz. The computational capabilities of the LEO and MEO satellites are set to 5 GHz and 10 GHz, respectively [25]. The effective switch capacitance is set at $\kappa = 10^{-28}$ Watt $\cdot \sec^3/\text{cycle}^3$. User transmission power is assumed to be 17 dBm with an antenna gain of 5 dBi, while the antenna gain for both LEO and MEO satellites is set at 20 dBi [25].

The simulation also considers a set of 100 users, randomly distributed within the area surrounding the target zone. The user-to-satellite channels are modelled by large-scale fading based on free-space path loss and small-scale fading, which follows a Rician distribution with a Rician factor of 10 [25]. Task sizes are randomly select a 1 or 2 Mbits and $\tau_u^{\rm th} = 3$ sec. The required processing cycles is 1000 cycles/bit The background noise density is set to $-174 \, \text{dBm/Hz}$ [25]. The optimization parameters α_1 and α_2 are both set to 0.1 to penalize packet blocking rates while balancing task delay and energy consumption. The simulation results are based on 500 independent Monte Carlo realizations where a subset of users is active following Poisson distribution with rate $\lambda = 5$. Because we focus on remote areas with limited terrestrial network availability, we consider two baseline scenarios in addition to the proposed hybrid MEO-LEO network: (1) a LEO-only network for communication and task offloading and (2) a standalone MEO (MEO-only) network.

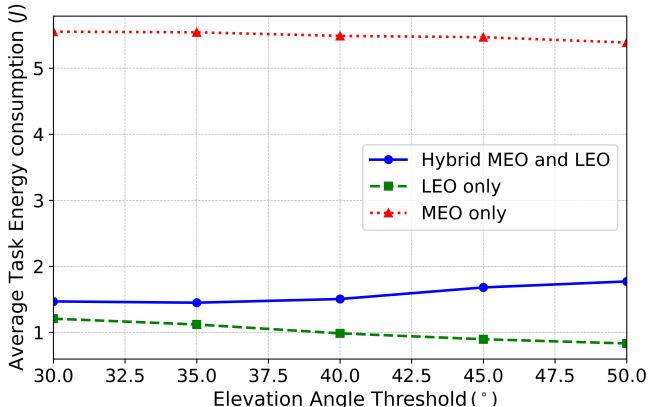
Fig. 3 presents the results of the proposed hybrid LEO-MEO architecture compared to using either MEO or LEO satellite networks independently. The task admission rate against the elevation angle threshold is shown in Fig. 3a. It is evident that the proposed hybrid LEO-MEO offloading scheme outperforms the baseline approaches, with the performance gain increasing as the elevation angle threshold rises, reaching up to 15% at an elevation angle threshold of 50° degrees compared to the LEO network. This can be justified by the decrease in the number of visible LEO satellites as the



(a) Admission rate vs elevation angle.



(b) Average delay vs elevation angle.



(c) Average energy consumption vs elevation angle.

Fig. 3: Numerical performance analysis.

elevation angle threshold increases. However, the number of visible MEO satellites decreases slightly due to their higher altitudes, which maintain higher elevation angles, which is also shown in the performance of the MEO network. Despite this, the hybrid architecture provides additional communication and computational paths, allowing more tasks to be admitted. It is also clear that using only LEO satellites results in a higher admission rate compared to using only MEO satellites. This is due to the higher path loss in MEO satellites compared to LEO networks, which limits the number of offloaded tasks given MEOs' limited frequency and computational resources.

Figs. 3b and 3c illustrate the average task delay and energy consumption against the elevation angle threshold. For the proposed scheme, the average delay and the energy consumption increase as the elevation angle threshold increases. This is because of the increased number of tasks offloaded to MEO satellites with higher transmission energy consumption. This is further supported by the behaviour of the MEO network, indicating that energy consumption is dominated by MEO transmission energy. Additionally, the LEO network experiences higher delay compared to the proposed hybrid scheme, up to 12% at 50°, as more tasks are allocated to fewer LEO satellites, resulting in increased transmission, propagation, and computational delays. This effect becomes clearer as the elevation angle increases, reducing the number of visible LEO satellites. It is worth noting that the MEO network exhibits a decrease in average delay as fewer tasks are admitted due to limited visible MEO satellites, leading to better utilization of computational resources.

VII. CONCLUSION

This paper addresses the task offloading problem in a hybrid LEO-MEO architecture to maximize the task admission rate while balancing energy consumption and delay, given specific delay requirements. As the formulated problem is a mixed-integer nonlinear program (MINLP), we apply disjunctive constraints and convex relaxation techniques to reformulate the problem into a convex form, which is readily solved using standard optimization tools. Through extensive simulations, we demonstrate that the proposed hybrid LEO-MEO architecture achieves an increase in admission rate by up to 15% and a reduction in average delay by up to 12% at an elevation angle threshold of 50° , compared to a LEO-only satellite network. These results underscore the potential of the proposed architecture to enhance service reliability in Arctic regions.

REFERENCES

- A. Iqbal *et al.*, "Empowering Non-Terrestrial Networks With Artificial Intelligence: A Survey," *IEEE Access*, vol. 11, pp. 100986–101006, Sep. 2023.
- [2] S. Mahboob and L. Liu, "Revolutionizing Future Connectivity: A Contemporary Survey on AI-Empowered Satellite-Based Non-Terrestrial Networks in 6G," *IEEE Commun. Surveys Tuts.*, vol. 26, no. 2, pp. 1279– 1321, 2024.
- [3] M. Giordani and M. Zorzi, "Non-Terrestrial Networks in the 6G Era: Challenges and Opportunities," *IEEE Netw.*, vol. 35, no. 2, pp. 244–251, Mar. 2021.
- [4] M. Harounabadi and T. Heyn, "Toward Integration of 6G-NTN to Terrestrial Mobile Networks: Research and Standardization Aspects," *IEEE Wireless Commun.*, vol. 30, no. 6, pp. 20–26, Dec. 2023.
- [5] Y. Mao, C. You, J. Zhang, K. Huang, and K. B. Letaief, "A Survey on Mobile Edge Computing: The Communication Perspective," *IEEE Commun. Surveys Tuts.*, vol. 19, no. 4, pp. 2322–2358, 2017.
- [6] S. Zarandi and H. Tabassum, "Delay Minimization in Sliced Multi-Cell Mobile Edge Computing (MEC) Systems," *IEEE Commun. Lett.*, vol. 25, no. 6, pp. 1964–1968, June 2021.
- [7] United Nations Human Rights Council, "The promotion, protection and enjoyment of human rights on the Internet," https://digitallibrary.un.org/record/3937534?v=pdf, Jul. 2016.
- [8] M. Almekhlafi, A. Lesage-Landry, and G. Karabulut Kurt, "Access Inequality in LEO Satellite Networks: A Case Study of High-Latitude Coverage in Northern Québec," *IEEE Open J. Veh. Technol.*, vol. 6, pp. 1613–1630, June 2025.

- [9] S. Map, "Satellite Map of Starlink and OneWeb," 2024. [Online]. Available: https://satellitemap.space/
- [10] Y. Sadovaya, O. Vikhrova, S. Andreev, and H. Yanikomeroglu, "Enhancing Service Continuity in Non-Terrestrial Networks via Multi-Connectivity Offloading," *IEEE Commun. Lett.*, pp. 1–1, Oct. 2024.
- [11] Q. Ren, O. Abbasi, G. Karabulut Kurt, H. Yanikomeroglu, and J. Chen, "Caching and Computation Offloading in High Altitude Platform Station (HAPS) Assisted Intelligent Transportation Systems," *IEEE Trans. Wireless Commun.*, vol. 21, no. 11, pp. 9010–9024, Nov. 2022.
- [12] X. Dai, Z. Xiao, H. Jiang, and J. C. S. Lui, "Uav-assisted task offloading in vehicular edge computing networks," *IEEE Trans. Mob. Comput.*, vol. 23, no. 4, pp. 2520–2534, April 2024.
- [13] A. Sacco, F. Esposito, G. Marchetto, and P. Montuschi, "A Self-Learning Strategy for Task Offloading in UAV Networks," *IEEE Trans. Veh. Technol.*, vol. 71, no. 4, pp. 4301–4311, April 2022.
- [14] N. Zhao, Z. Ye, Y. Pei, Y.-C. Liang, and D. Niyato, "Multi-Agent Deep Reinforcement Learning for Task Offloading in UAV-Assisted Mobile Edge Computing," *IEEE Trans. Wireless Commun.*, vol. 21, no. 9, pp. 6949–6960, Sept. 2022.
- [15] M. Zhang, Z. Su, Q. Xu, Y. Qi, and D. Fang, "Energy-Efficient Task Offloading in UAV-RIS-Assisted Mobile Edge Computing with NOMA," in *Proc. IEEE INFOCOM*, Vancouver, BC, Canada, Aug. 2024, pp. 01– 06
- [16] M. Chen and Y. Hao, "Task Offloading for Mobile Edge Computing in Software Defined Ultra-Dense Network," *IEEE J. Sel. Areas Commun.*, vol. 36, no. 3, pp. 587–597, Mar. 2018.
- [17] Q. Ren, O. Abbasi, G. Karabulut Kurt, H. Yanikomeroglu, and J. Chen, "Handoff-Aware Distributed Computing in High Altitude Platform Station (HAPS)—Assisted Vehicular Networks," *IEEE Trans. Wireless Commun.*, vol. 22, no. 12, pp. 8814–8827, Dec. 2023.
- [18] I. Leyva-Mayorga et al., "Satellite Edge Computing for RealTime and VeryHigh Resolution Earth Observation," IEEE Trans. Wireless Commun., vol. 71, no. 10, pp. 6180–6194, Oct. 2023.
- [19] T. Lyu, Y. Xu, F. Liu, H. Xu, and Z. Han, "Task Offloading and Resource Allocation for Satellite-Terrestrial Integrated Networks," *IEEE Internet Things J.*, vol. 12, no. 1, pp. 262–275, Jan. 2025.
- [20] J. Zhou, D. Tian, Z. Sheng, X. Duan, and X. Shen, "Distributed Task Offloading Optimization With Queueing Dynamics in Multiagent Mobile-Edge Computing Networks," *IEEE Internet Things J.*, vol. 8, no. 15, pp. 12311–12328, Aug. 2021.
- [21] L. Zhao et al., "QoS-Aware Multi-Hop Task Offloading in Satellite-Terrestrial Edge Networks," *IEEE Internet Things J.*, vol. 11, no. 19, pp. 31453–31466, Oct. 2024.
- [22] S. S. Shinde, D. Naseh, and D. Tarchi, "In-Space Computation Offloading for Multi-layer LEO Constellations," in *Proc. IEEE EW 2023*, Rome, Italy, Mar. 2023, pp. 82–89.
- [23] H. Wu, X. Yang, and Z. Bu, "Task Offloading With Service Migration for Satellite Edge Computing: A Deep Reinforcement Learning Approach," *IEEE Access*, vol. 12, pp. 25844–25856, 2024.
- [24] M. Y. Abdelsadek, G. Karabulut Kurt, and H. Yanikomeroglu, "Distributed Massive MIMO for LEO Satellite Networks," *IEEE OJ-COMS*, vol. 3, pp. 2162–2177, Nov. 2022.
- [25] C. Ding et al., "Joint Optimization of Transmission and Computation Resources for Satellite and High Altitude Platform Assisted Edge Computing," *IEEE Trans. Wireless Commun.*, vol. 21, no. 2, pp. 1362– 1377, Feb. 2022.
- [26] D. Bhattacharjee, P. G. Madoery, A. U. Chaudhry, H. Yanikomeroglu, G. Karabulut Kurt, P. Hu, K. Ahmed, and S. Martel, "On-Demand Routing in LEO Mega-Constellations With Dynamic Laser Inter-Satellite Links," *IEEE Trans. Aero. Elect. Sys.*, vol. 60, no. 5, pp. 7089–7105, 2024.
- [27] S. Diamond and S. Boyd, "CVXPY: A Python-embedded modeling language for convex optimization," *Journal of Machine Learning Research*, vol. 17, no. 83, pp. 1–5, 2016.
- [28] Gurobi Optimization, LLC, "Gurobi Optimizer Reference Manual," 2024. [Online]. Available: https://www.gurobi.com
- [29] M. Samir, S. Sharafeddine, C. Assi, T. M. Nguyen, and A. Ghrayeb, "Trajectory Planning and Resource Allocation of Multiple UAVs for Data Delivery in Vehicular Networks," *IEEE Commun. Lett.*, vol. 1, no. 3, pp. 107–110, Sept. 2019.
- [30] B. Rhodes, "Skyfield: High precision research-grade positions for planets and Earth satellites generator," *Astrophysics Source Code Library*, pp. ascl–1907, 2019.
- [31] T. Kelso, "Celestrak," 2024. [Online]. Available: https://celestrak.com/